

Spatial Compressed Sensing for Field Reconstruction in Full-Scale Structural Systems

A. Jesus PhD, CEng, FHEA
Loughborough University, School of Architecture, Building & Civil
Engineering, Epinal Way, Loughborough LE11 3TU, UK

S. M. Mojtabaei PhD, CEng, FHEA
Loughborough University, School of Architecture, Building & Civil
Engineering, Epinal Way, Loughborough LE11 3TU, UK

High dimensional systems, such as large civil infrastructure, exhibit fundamental patterns in space and time which can be exploited for efficient data acquisition, reconstruction, identification and damage detection. This study numerically investigates the applicability of compressed sensing (CS) theory to reconstruct the static displacement field of a multi-storey building using a small number of displacement samples. A full-scale Finite Element (FE) model of the building, developed using Opensees software, is used to capture its static displacement field and vibratory mode shapes, which serve as a tailored physics-guided basis. A sample of displacement data was then randomly selected, aiming to reconstruct the entire displacement field. The results demonstrate that achieving a reliable full-scale reconstruction is feasible with only approximately one percent of the total degrees of freedom in the original model. This highlights the effectiveness of the CS paradigm in accurately reconstructing various measurement fields within buildings, emphasizing its potential to enhance the efficiency of information extraction from spatially distributed sensor networks.

1. Introduction

Structural systems are often large in scale and exhibit a complex interaction with the surrounding environment, which is challenging to both measure accurately or model reliably. Measurements are used jointly with machine learning techniques to extract information relevant to identify the performance of a structure and the onset of damage, also known as Structural Health Monitoring (SHM) [Farrar and Worden \(2007\)](#). On the other hand, experimentally validated models can be used to aid this task [Jesus et al. \(2019, 2017\)](#) or also to predict the state of the structure at any future point in time; and ultimately to estimate its remaining useful life [Le et al. \(2016\)](#).

The ability to capture how such systems behave globally from a set of local measurements is known in signal processing and machine learning literature as reconstruction. For example, reconstructing the displacement or stress fields within a structure

helps minimise the required number of sensors while allowing for the identification of potentially vulnerable areas. Environmental conditions influencing a structure, such as temperature and moisture content, are also extremely relevant to reconstruct given their large influence in mechanical properties and their wide spatio-temporal variability.

One of the most efficient and recent reconstruction techniques that has gathered considerable interest in the scientific community is compressed sensing (CS) [Candes and Wakin \(2008\)](#). Its efficiency stems from the fact that it allows to reliably reconstruct many signals with a sub-Nyquist sampling rate, which has been the traditional standard for perfect signal reconstruction. Since its establishment, numerous applications have been proposed, such as reconstruction of acceleration time-series for low-power wireless sensor network deployment in operational modal analysis applications (OMA) [Gkoktsi and Giaralis \(2019, 2017\)](#);

[Tau Siesakul et al. \(2015\)](#). Wireless accelerometers are affordable and operationally convenient for OMA, but require high sampling rates and most of their energy is spent quickly during the act of signal acquisition when at the Nyquist sampling rate.

Other examples of SHM applications using CS can be seen in Mascareñas et al [Mascareñas et al. \(2013\)](#) or Jana and Nagarajaiah [Jana and Nagarajaiah \(2022\)](#). In these works signals are reconstructed in the time domain using a generic Fourier or wavelet basis, or alternatively using the underlying physics to form an analytical reduced order model basis. The former is widely applicable but requires a larger number of measurements, whilst the latter requires less measurements but is limited in its applicability to full-scale structures, since a continuous analytic structural model typically only exists for simple components, e.g. slabs, beams, columns, etc.

Another technique commonly used with CS, which forms a suitable basis when the target field is difficult to model analytically, is proper orthogonal decomposition (POD). Two such examples are reconstruction of a temperature field of a steam turbine based on finite element simulations, as in [Jiang et al. \(2022\)](#), or reconstruction of temperature and pressure field during fluid flow using POD, as investigated by Matulis and Bindra [Matulis and Bindra \(2024\)](#). The POD is also used to simplify highly nonlinear hygrothermal fields [Hou et al. \(2019\)](#), although its reconstruction remains unexplored.

The contribution of this work is to demonstrate how a full-scale static displacement field can be reconstructed through CS. To achieve this, a structure's vibratory mode shapes, readily obtained from an FE model, serve as the basis for reconstruction. Static displacement field reconstruction has been demonstrated previously, as evidenced by [Yan et al. \(2022\)](#) or [Rapp et al. \(2009\)](#) for two-dimensional plates. However, these reconstructions are not full-scale and unlike the aforementioned work we are not using POD, but rather the actual mode shapes obtained directly from FE, resulting in a reduced computational effort and fewer number of required measurements. Additionally, the optimal number of modes and measurements are parametrically analysed, along with their interaction with the associated reconstruction error.

In this study, a five-storey reinforced concrete (RC) building is modeled in FE Opensees software. Both modal and static linear analyses are conducted on the building FE model. A CS reconstruction method is then developed to reconstruct the displacement field under gravity load, followed by numerical tests to assess the reconstruction performance in terms of both accuracy and computational efficiency.

2. Compressed sensing for full-scale field reconstruction

2.1. Sparse signal representation and recovery using convex optimisation

This section describes the formulation of the proposed framework, considering the applicability of compressed sensing theory for full-scale field reconstruction.

Consider a signal $\mathbf{y} \in \mathbb{R}^{N \times 1}$, which is discretised in space. The signal is assumed to be K -sparse/compressible in an orthonormal basis matrix $\Psi \in \mathbb{R}^{N \times N}$, which describes a field of a quasi-static process within a structure, e.g. displacement, temperature, stress or moisture content. The sparse representation of the signal is given by

$$(1) \quad \mathbf{y} = \Psi \mathbf{s}$$

where \mathbf{s} is a sparse vector collecting the K non-zero coefficients of the considered signal, where $K \ll N$, in the established basis. According to compressed sensing theory [Donoho \(2006\)](#); [Candes and Wakin \(2008\)](#), under certain conditions these coefficients can be estimated from a set of randomly sampled measurements of \mathbf{y} , denoted as $\mathbf{z} \in \mathbb{R}^M$ with size $M \ll N$ and $K < M$. Further, CS asserts that for an increasing number of measurements the original signal can be recovered with overwhelming probability. The observation equation, establishing the samples that will be acquired, is expressed as

$$(2) \quad \mathbf{z} = \mathbf{C} \mathbf{y},$$

where $\mathbf{C} \in \mathbb{R}^{M \times N}$ is the so-called measurement matrix, which has to be carefully chosen to be as *incoherent* with respect to Ψ as possible. In this work \mathbf{C} is based on a uniformly random selection of the N available entries of the original signal \mathbf{y} , noting that each measurement is unique, i.e. no multiple measurements of the same entry are allowed. This is a common choice in CS

applications with proved incoherency for a diverse number of bases [Sankaranarayanan and Baraniuk \(2014\)](#); [Candes and Wakin \(2008\)](#).

Combining Eqs. (1) and (2) results in the following undetermined linear system of equations

$$(3) \quad \mathbf{z} = \mathbf{C}\Psi\mathbf{s} = \Theta\mathbf{s}.$$

There are infinitely many solutions to the above set of equations, i.e., vectors \mathbf{s} that provide a good match with the measurements \mathbf{z} , and finding the correct one was traditionally a combinatorially hard optimisation problem.

A particular solution, that faithfully reconstructs the original signal \mathbf{y} without an exponential increase of computational requirement, is to obtain the sparsest coefficient vector \mathbf{s} , i.e. with the smallest sum of the absolute values of the vector, that is consistent with Eq. (3). In practice, this is enforced by using the ℓ_1 norm.

Such particular solution is obtained by solving a convex optimisation problem, defined for the noiseless case as

$$(4) \quad \hat{\mathbf{s}} = \arg \min \|\mathbf{s}\|_1 \quad \text{subject to} \quad \mathbf{z} = \Theta\mathbf{s}$$

where $\|\cdot\|_1$ denotes the ℓ_1 norm and $\hat{\mathbf{s}}$ is an estimate of the coefficients. There are several methods capable of efficiently solving (4) including when in the presence of noisy measurements, e.g. LASSO or orthogonal basis matching pursuit [Tibshirani \(1996\)](#); [Chen et al. \(1998\)](#). The open source package CVXPY [Diamond and Boyd \(2016\)](#) is used in this work to solve this problem using the numerical splitting conic solver (SCS) [O'Donoghue et al. \(2016\)](#).

2.2. Basis vectors from FE modelled vibratory mode shapes

In the formulation discussed in the previous section, choosing an appropriate basis matrix Ψ plays a critical role, as it needs to be able to represent \mathbf{y} sparsely, and it needs to be orthonormal. Most of existent literature adopt one of two strategies:

- use of a *universal basis*, including Fourier, wavelet or discrete-cosine bases, which are generic and adaptable to a number of problems, such as reconstruction of vibration time series, audio signals or 2D images;

- use of a *tailored basis*, obtained from POD of a problem's partial differential equations or via the singular value decomposition (SVD) of relevant data (if available). This type of basis is less flexible but results in a physically interpretable spatio-temporal decomposition and reconstruction of a target field with less measurements than with a universal basis.

In this work, the latter type of basis is used, considering vibratory mode shapes of a structure as a basis of its displacement field, since they represent the spatial dependency of the motion of a structure, and allow for an approximation of the true solution for an increasing number of modes. In the following text the mode shapes are contextualised within structural dynamics and their orthonormalisation process is detailed, although it is stressed that they will be used to approximate a static displacement field.

The equations of motion for an undamped unforced multiple degree of freedom (MDOF) system can be written in matrix form as

$$(5) \quad \mathbf{M}\ddot{\mathbf{y}}(t) + \mathbf{K}\mathbf{y}(t) = \mathbf{0},$$

where \mathbf{M} , and \mathbf{K} are \mathbb{R}^n mass and stiffness matrices, $\ddot{\mathbf{y}}$ and \mathbf{y} are $\mathbb{R}^{n \times 1}$ time-dependent vectors of acceleration and displacement at each of the n degrees of freedom (DOF), respectively. Commonly, a solution to the equation of motion is obtained by coordinate transformation into modal space and truncation of the number of modes $m \leq n$

$$(6) \quad \mathbf{y}(t) = \Phi\mathbf{q}(t),$$

where $\Phi \in \mathbb{R}^{n \times m}$ is a mode shape matrix containing m mode shapes $\Phi = [\Phi_1, \Phi_2, \dots, \Phi_m]$ and $\mathbf{q}(t) \in \mathbb{R}^{m \times 1}$ is a modal coordinate vector. This separation of the response into a pattern in space and time, combined with truncation and subsequent modal superposition is intuitive and appealing from a physical point of view.

Mode shapes are typically normalised so that they are orthogonal with respect to the mass matrix or unity normalised. In the context of the CS framework presented in Section 2 they need to be orthonormal, and this can be achieved by taking the SVD of the truncated mode shape matrix

$$(7) \quad \Phi = \mathbf{U}\Sigma\mathbf{V}^T$$

where $\mathbf{U} \in \mathbb{R}^{n \times n}$ and $\mathbf{V} \in \mathbb{R}^{m \times m}$ are real orthogonal matrices, and $\mathbf{\Sigma} = \begin{bmatrix} \hat{\mathbf{\Sigma}} & \mathbf{0} \end{bmatrix}^T \in \mathbb{R}^{n \times m}$ is a rectangular diagonal matrix, whose singular values $\hat{\mathbf{\Sigma}}$ in the diagonal are to be replaced with ones. The resulting basis matrix is then given by

$$(8) \quad \mathbf{\Psi} = \mathbf{U} \begin{bmatrix} \mathbf{I}_m \\ \mathbf{0} \end{bmatrix} \mathbf{V}^T$$

where \mathbf{I}_m is the m^{th} identity matrix.

3. Five storey RC building FE model

3.1. Geometry, boundary conditions and modelling aspects

To validate the proposed compressed sensing framework, an Openses FE model of a 5-storey plan-irregular building, modelled after an actual building located in Turkey, has been developed and is presented in this section. The plan view and elevation of the building are shown in Fig. 1. Fibre-section displacement based

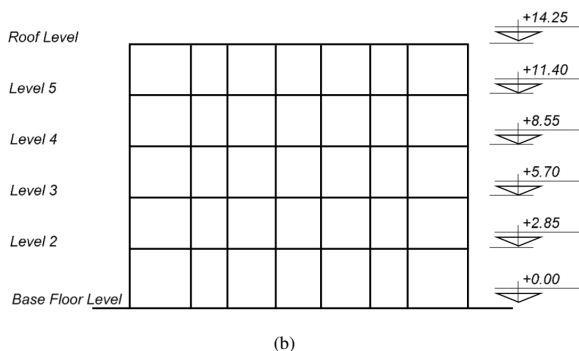
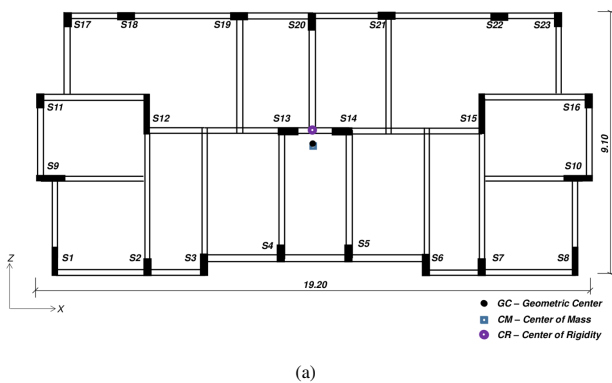


Figure 1. Plan (a) and elevation (b) view of a 5 storey RC building, adapted from Hussain (2016).

diaphragms. The columns are discretised into five elements and the beams into a minimum of three elements, depending on their lengths. Their section views are represented in Fig. 2 and Fig. 3

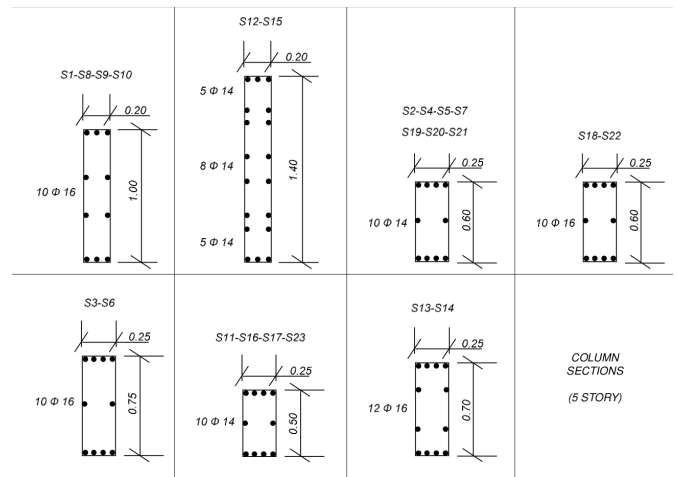


Figure 2. Column sections, dimensions in m and reinforcement in mm. Figure reproduced from Hussain (2016).

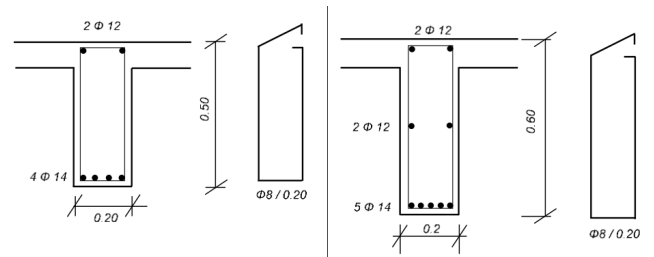


Figure 3. Beam sections, dimensions in m and reinforcement in mm. Figure reproduced from Hussain (2016).

A brief synopsis of the material properties of concrete and steel is provided in Tables 1 and Table 2.

Material parameters	Unit	Concrete
Concrete compressive strength at 28 days	kPa	-17502
Concrete tensile strength	kPa	1394
Density	kg/m ³	2400

Table 1. Concrete material properties

beam-column elements are used to model the beams and columns of the building, respectively, whilst the floors are modelled as rigid

Material parameters	Unit	Reinforcing Steel
Steel yield strength	kPa	371000
Initial elastic tangent	kPa	200000000
Strain hardening parameter	kPa	1394
Density	kg/m ³	7850

Table 2. Reinforcing steel material properties

and the corresponding Opensees model and deflected shape are shown in Fig. 4. The deflected shape is obtained from a linear static analysis under the building self-weight.

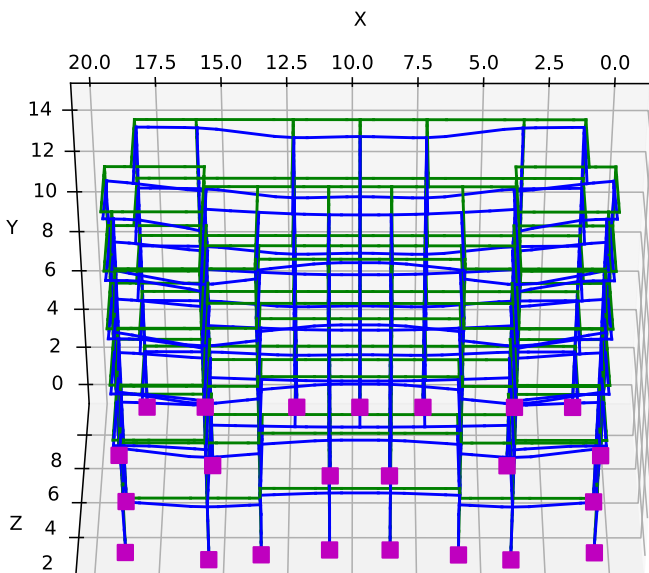


Figure 4. 5 storey RC building Opensees model and deformed shape, dimensions in m with a scaling factor of 20.

3.2. Modal analysis

A modal analysis has also been performed and the first three mass-normalised mode shapes of the building, lateral in both directions and torsional, are shown in Fig. 5. In total, $m = 56$ modes have been extracted from Opensees, each with $n = 3234$ translational degrees of freedom, and been made orthonormal as detailed in Section 2.2.

To ensure that this number suffices to reconstruct the displacement field, the modal participation mass ratios in each axis are plotted in Fig. 6. As it can be observed, above 30 modes the mass ratios are over 90% in all three directions, thus capturing most of the

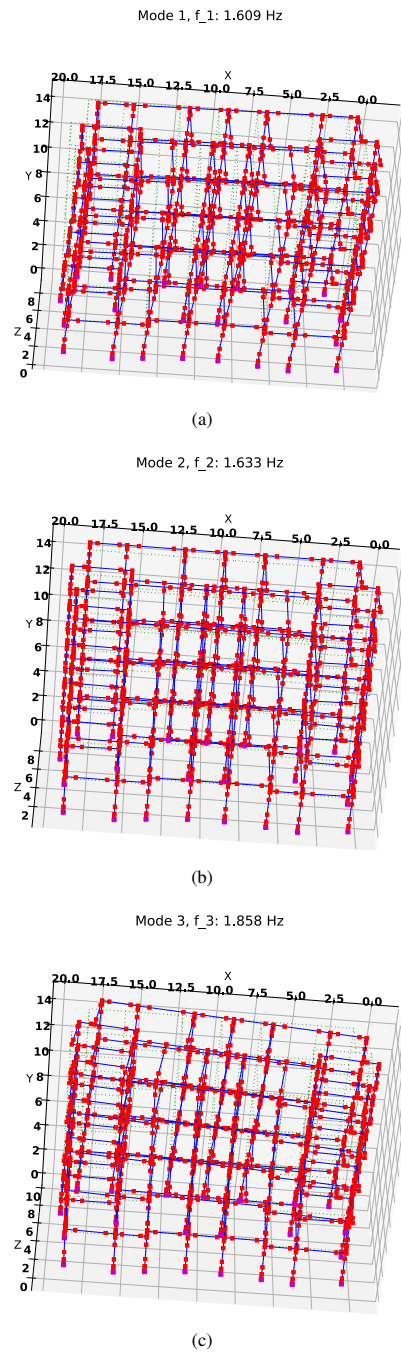


Figure 5. First three mass-normalised mode shapes, scaling factor of 20.

available energy, and with 56 modes more than 96% of all mass is mobilised.

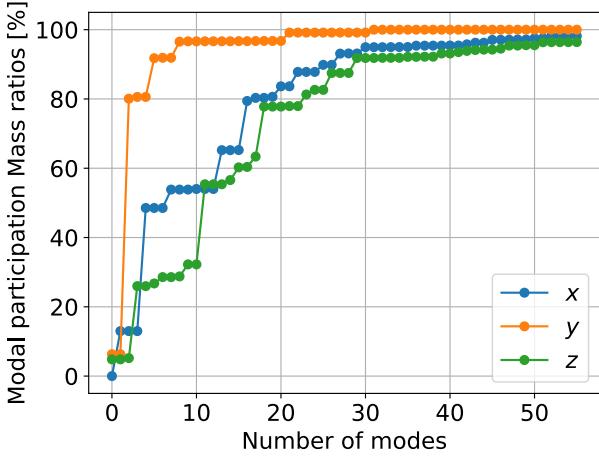


Figure 6. Modal participation mass ratios in translational directions.

Additional information regarding section profiles, material properties and other constructive details of the building can be found elsewhere Hussain (2016); Bhatt and Bento (2014).

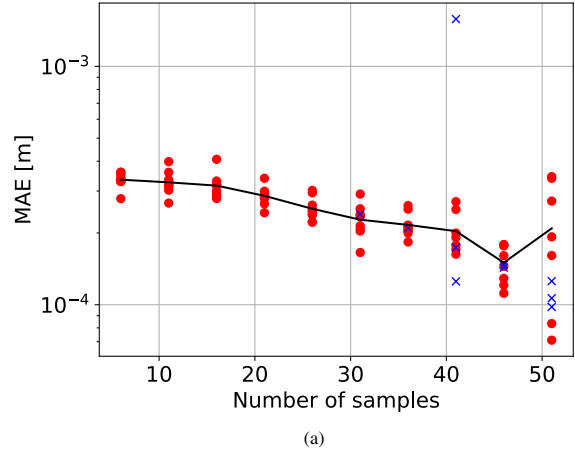
4. Numerical verification

To compare the performance of the full-field reconstruction, two metrics have been assessed against an increasing number of samples: the mean absolute error (MAE) and the mean squared error (MSE). The MAE and MSE are defined as

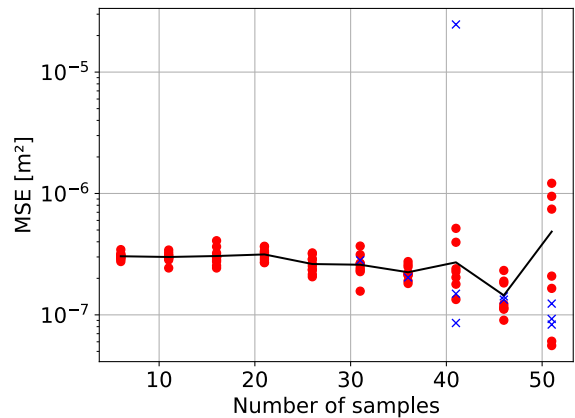
$$(9) \quad MAE = \frac{\sum_{i=1}^n |\hat{y}_i - y_i|}{n} \quad MSE = \frac{\sum_{i=1}^n (\hat{y}_i - y_i)^2}{n}$$

where \hat{y}_i and y_i are the displacements of the i^{th} DOF, reconstructed and actual, respectively.

Next, the capability to reconstruct the displacement field of the building has been parametrically analysed, considering a number of samples from 6 up to 56 in increments of 5, i.e., within a range of $M = [6, 11, 16, 21, 26, 31, 36, 41, 46, 51, 56]$. The selected number of samples correspond to the following compression ratios $M/N = 0.18\%, 0.34\%, 0.49\%, 0.64\%, 0.80\%, 0.95\%, 1.11\%, 1.26\%, 1.42\%, 1.57\%$, and 10 reconstructions were performed at each compression ratio, to account for the variability of the procedure. The results are shown in Fig. 7, where the red circles and blue crosses represent runs in which the optimisation process has converged or not, respectively. If the solver does not converge it returns the best 19 results attained



(a)



(b)

Figure 7. Mean absolute (a) and squared (b) reconstruction errors. Red circles and blue crosses are successful and unsuccessful optimisation runs, respectively, and the black solid line is the average trendline for successful optimisation runs.

during the optimisation, whose average is plotted as a blue cross in the figures.

As can be observed, increasing the number of samples decreases the reconstruction errors, although when the number of samples approaches the maximum number of available modes the variance of the error tends to increase, and there are some unsuccessful optimisation runs. The reason is that when, $M \approx N$, Eq. (3) is a determinate rather than undetermined system, as typically assumed in CS. In this case, the solution could instead be obtained by

computing the inverse or the pseudo-inverse of matrix Θ and multiplying it by the sampled measurement vector.

Regarding the performance of the reconstruction, and as shown in Fig. 7(a), the average absolute error is between half and a tenth of a millimeter for only 6 up to 56 samples, or a compression ratio between 0.18 % and 1.73 %. This is a consequence of the suitable basis that has been used, combined with the efficiency of the CS technique.

Next, the reconstruction of the displacement field of the building at a 0.95 % compression level is illustrated in Fig. 8. The original displacement signal in each of the three directions is shown in Fig. 8(a) as well as the samples (red circles). The coefficients in the vector s are shown in the bar chart of Fig. 8(b), where it is clear that the obtained solution is sparse. A 3D visualisation of the original and reconstructed field is shown in Fig. 9. In this figure, a large scaling factor has been used to overexaggerate the differences between the two fields, most notably at the top of the building.

Finally, the computational time of the above 50 runs is reported as 48.305 s which is exceptionally fast: on average each optimisation run took less than 1 s.

5. Conclusions and future work

In this study, a full-scale reconstruction of the displacement field, based on the compressed sensing technique, of a reinforced concrete building has been analysed. The vibratory mode shapes, which can be typically obtained from a simple FE modal analysis, have been used as a physics-guided basis for reconstruction of the field. The conclusions of the present work and future research avenues can be summarised as follows:

- Under the assumption of noiseless measurements and no modelling error, it is possible to obtain a faithful reconstruction, with compression ratios at around one percent and errors at the tenth of a millimeter scale;
- The computational effort is negligible, with each optimisation requiring on average less than a second. It should be noted, however, that in some instances the optimisation might not converge, particularly when the number of measurements is close to the number of modes;

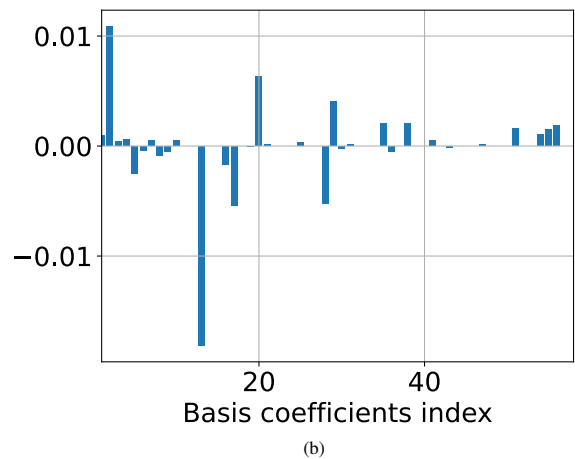
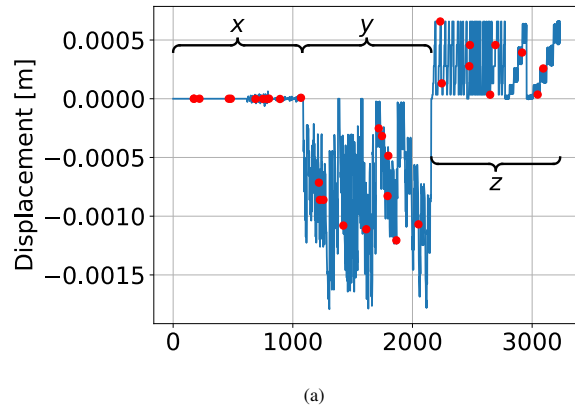


Figure 8. Original displacement field signal (a) with 31 samples (red circles), and corresponding sparse coefficient vector (b).

- The framework is simple to implement and showcases how reconstruction using compressed sensing for a full-scale structure can be achieved;
- Future work includes expanding the framework to account for noisy measurements, validation with experimental data, and the ability to reconstruct more challenging full-scale fields where a spatio-temporal physics-guided basis might not be readily available, such as temperature and moisture content transport and ingress. This could be achieved using an SVD basis.

Acknowledgements

The first author acknowledges provision of a first version of the Opensees FE model by Professor André Barbosa, Oregon State University.

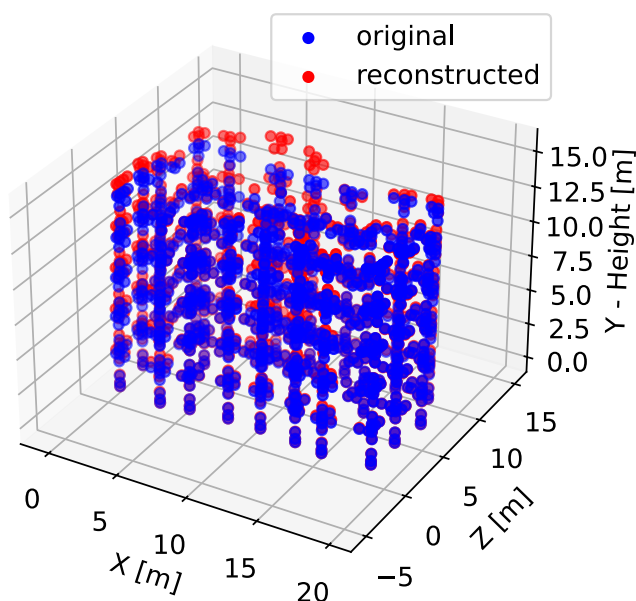


Figure 9. 3D view of original and reconstructed displacement field (c), scaling factor of 1000.

Data availability

The source code, raw and processed data required to reproduce these findings will be made available upon request.

REFERENCES

Bhatt, C. and Bento, R. (2014). "The extended adaptive capacity spectrum method for the seismic assessment of plan-asymmetric buildings." *Earthquake Spectra*, 30(2), 683–703.

Candes, E. and Wakin, M. (2008). "An Introduction To Compressive Sampling." *IEEE Signal Processing Magazine*, 25(2), 21–30.

Chen, S. S., Donoho, D. L., and Saunders, M. A. (1998). "Atomic decomposition by basis pursuit." *SIAM Journal on Scientific Computing*, 20(1), 33–61.

Diamond, S. and Boyd, S. (2016). "Cvxpy: a python-embedded modeling language for convex optimization." *nil, nil(nil), nil*.

Donoho, D. (2006). "Compressed sensing." *IEEE Transactions on Information Theory*, 52(4), 1289–1306.

Farrar, C. R. and Worden, K. (2007). "An introduction to structural health monitoring." *Philosophical Transactions of the Royal Society A: Mathematical, Physical and Engineering Sciences*, 365(1851), 303–315.

Gkoktsi, K. and Giaralis, A. (2017). "Assessment of sub-Nyquist deterministic and random data sampling techniques for operational modal analysis." *Structural Health Monitoring: An International Journal*, 16(5), 630–646.

Gkoktsi, K. and Giaralis, A. (2019). "A multi-sensor sub-Nyquist power spectrum blind sampling approach for low-power wireless sensors in operational modal analysis applications." *Mechanical Systems and Signal Processing*, 116, 879–899.

Hou, T., Roels, S., and Janssen, H. (2019). "The use of proper orthogonal decomposition for the simulation of highly nonlinear hygrothermal performance." *MATEC Web of Conferences*, 282(nil), 02018.

Hussain, S. (2016). "Evaluation of seismic response directional combination rules for existing plan irregular reinforced concrete buildings." M.S. thesis, Oregon State University, Oregon State University.

Jana, D. and Nagarajaiah, S. (2022). "Physics-guided real-time full-field vibration response estimation from sparse measurements using compressive sensing." *Sensors*, 23(1), 384.

Jesus, A., Brommer, P., Westgate, R., Koo, K., Brownjohn, J., and Laory, I. (2019). "Modular Bayesian damage detection for complex civil infrastructure." *Journal of Civil Structural Health Monitoring*, 9(2), 201–215.

Jesus, A., Brommer, P., Zhu, Y., and Laory, I. (2017). "Comprehensive Bayesian structural identification using temperature variation." *Engineering Structures*, 141, 75–82.

Jiang, G., Kang, M., Cai, Z., Wang, H., Liu, Y., and Wang, W. (2022). "Online reconstruction of 3d temperature field fused with pod-based reduced order approach and sparse sensor data." *International Journal of Thermal Sciences*, 175(nil), 107489.

Le, T. T., Chatelain, F., and Bérenguer, C. (2016). "Multi-branch hidden markov models for remaining useful life estimation of systems under multiple deterioration modes." *Proceedings of the Institution of Mechanical Engineers, Part O: Journal of Risk and Reliability*, 230(5), 473–484.

Mascareñas, D., Cattaneo, A., Theiler, J., and Farrar, C. (2013). "Compressed sensing techniques for detecting damage in structures." *Structural Health Monitoring: An International Journal*, 12(4), 325–338.

Matulis, J. and Bindra, H. (2024). "Thermal field reconstruction and compressive sensing using proper orthogonal decomposition." *Frontiers in Energy Research*, 12(nil), nil.

O'Donoghue, B., Chu, E., Parikh, N., and Boyd, S. (2016). "Conic optimization via operator splitting and homogeneous self-dual embedding." *Journal of Optimization Theory and Applications*, 169(3), 1042–1068.

Rapp, S., Kang, L.-H., Han, J.-H., Mueller, U. C., and Baier, H. (2009). "Displacement field estimation for a two-dimensional structure using fiber bragg grating sensors." *Smart Materials and Structures*, 18(2), 025006.

Sankaranarayanan, A. C. and Baraniuk, R. G. (2014). *Computer Vision: A Reference Guide*. Springer US, Boston, MA, Chapter Compressive Sensing, 132–136.

Tau Siesakul, B., Gkoktsi, K., and Giaralis, A. (2015). "Compressive power spectrum sensing for vibration-based output-only system identification of structural systems in the presence of noise." *SPIE Sensing Technology + Applications*, F. Ahmad, ed., Baltimore, Maryland, United States, 94840K (May).

Tibshirani, R. (1996). "Regression shrinkage and selection via the lasso." *Journal of the Royal Statistical Society: Series B (Methodological)*, 58(1), 267–288.

Yan, J., Cheng, Y., Zhang, L., Li, Z., Xu, T., Zhang, F., Jiang, M., and Sui, Q. (2022). "Displacement field reconstruction technique for plate-like structures based on model superposition method." *Measurement and Control*, 56(3-4), 654–667.